

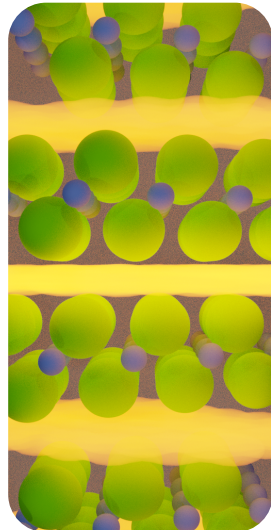
# LAYERED ELECTRIDES

## What They Are, What They Do, and What Can They Do

Adrian F. Rumson

Department of Chemistry  
Dalhousie University

University of Cambridge  
June, 2025



# Acknowledgements



Semiconductor  
Research  
Corporation



**NSERC**  
**CRSNG**



**ACENET**  
accelerate discovery



**NOVA SCOTIA**  
**NOUVELLE-ÉCOSSE**



**Digital Research  
Alliance** of Canada

**Alliance de recherche  
numérique** du Canada



**DALHOUSIE**  
UNIVERSITY

Introduction  
oooooooooooo

Thermal Expansion  
oooooooooooo

2D Semiconductors  
oooooooooooooooooooo

Conclusions  
o

## Introduction

## Thermal Expansion

## 2D Semiconductors

## Conclusions

Introduction  
oooooooooooo

Thermal Expansion  
oooooooooooo

2D Semiconductors  
oooooooooooooooooooo

Conclusions  
o

## Introduction

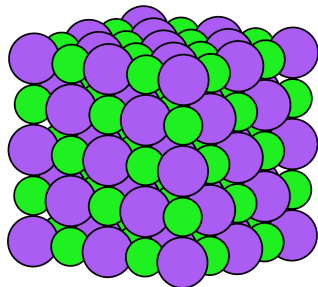
## Thermal Expansion

## 2D Semiconductors

## Conclusions

# Motivation: Ionic Materials

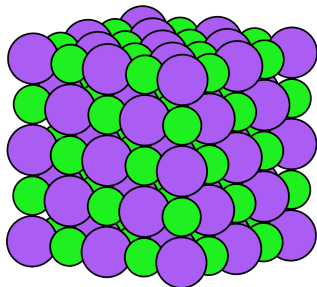
Consider NaCl:



Simple cubic lattice ( $Fm\bar{3}m$ ) composed of sodium cations and chloride anions:  
 $[Na^+][Cl^-]$

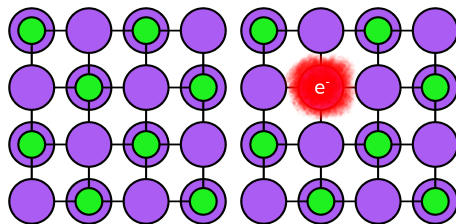
# Motivation: Ionic Materials

Consider NaCl:



Simple cubic lattice ( $Fm\bar{3}m$ ) composed of sodium cations and chloride anions:  
 $[Na^+][Cl^-]$

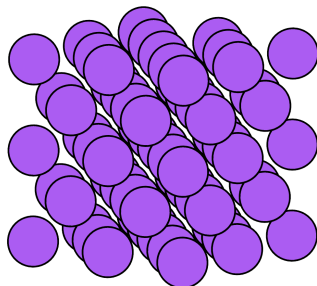
F-centers (*Farbzentrum*):



A crystallographic defect where an anion's position is vacant, but its electron(s) remain.

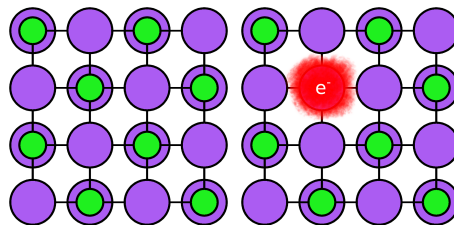
# Motivation: Ionic Materials

What if every anion was an F-center?



That would leave you with an ionic crystal of sodium  $[\text{Na}^+]:\text{e}^-$ .

F-centers (*Farbzentrum*):

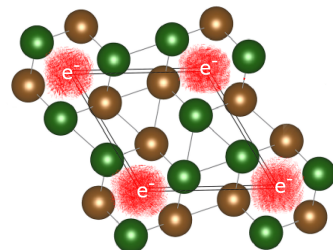


A crystallographic defect where an anion's position is vacant, but its electron(s) remain.

## Electride

**DEFINITION:** An ionic material where a localized electron acts in the place of an anion.

Sodium metal, under extreme conditions (250–350 GPa, 710–1900 K), becomes an electride.



Other materials can exhibit electride character under ambient conditions.

- $[\text{Ca}_{24}\text{Al}_{28}\text{O}_{64}]^{4+} : 4\text{e}^-$
  - $[\text{AE}_2\text{Pn}]^+ : \text{e}^-$ ,  $[\text{M}_2\text{C}]^{2+} : 2\text{e}^-$

Electrides are often notated as neutral, e.g.  $\text{Ba}_2\text{N}$ .

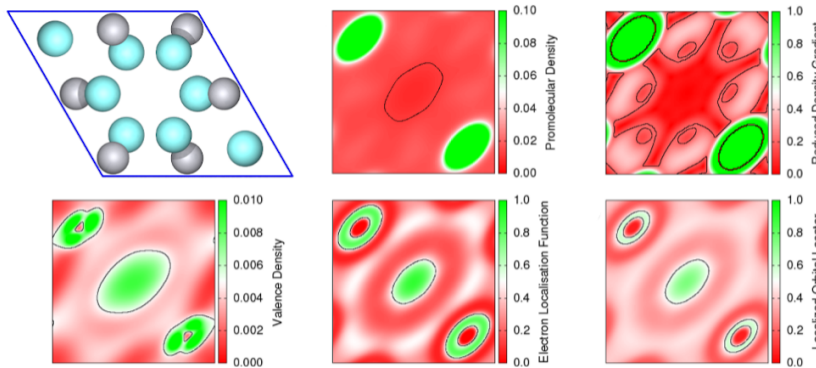
Electride character is often only recognized years or decades post initial synthesis.

How are electrides identified?

Some electrides can be identified with NMR or other experimental methods.



Most electrides are identified with computational visualization methods. (*viz.*  $\text{Y}_5\text{Si}_3$ )



ELF and ILDOS

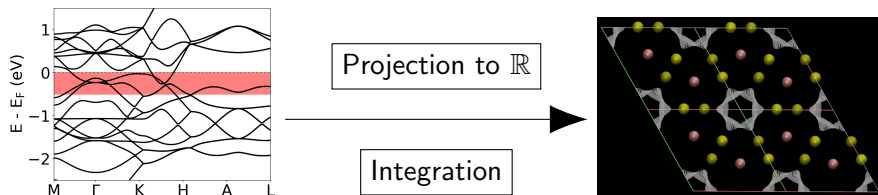
Two popular methods for visualization for identifying of electrides are the *electron localization function* (ELF):

$$D_\sigma(\mathbf{r}) = \tau_\sigma(\mathbf{r}) - \frac{1}{4} \frac{(\nabla \rho_\sigma(\mathbf{r}))^2}{\rho_\sigma(\mathbf{r})}$$

$$D_\sigma^{\text{UEG}}(\mathbf{r}) = \frac{3}{5} (6\pi^2)^{2/3} \rho_\sigma^{5/3}(\mathbf{r})$$

$$\text{ELF}(\mathbf{r}) = \frac{1}{1 + \left( \frac{D_\sigma(\mathbf{r})}{D_{\sigma}^{\text{UEG}}(\mathbf{r})} \right)^2}$$

and the *Integrated Local Density of States* (ILDOS):

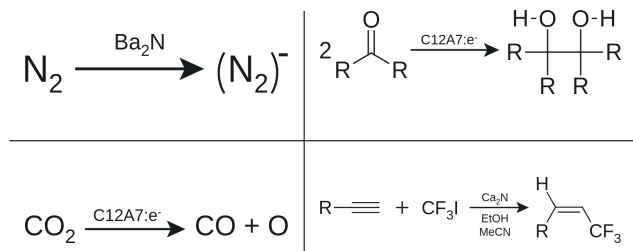


## What can they do?

Electrides are powerful reducing agents/have a very low work function.

## Chemical Applications:

- Nitrogen splitting ( $E_A$  of 35 kJ/mol *comparari* 108 kJ/mol with Ru/MgO)<sup>1</sup>
  - CO<sub>2</sub> splitting<sup>2</sup>
  - Pinacol coupling<sup>3</sup>
  - Hydrotrifluoromethylation of alkenes and alkynes<sup>4</sup>



[1] Zhang et al., *J Am. Chem. Soc.*, 2023, 145, 24482

[2] Toda et al., *Nat. Commun.*, 2013, 4, 2378.

[3] Buchammaga *et al.*, *Org. Lett.*, **2007**, *9*, 2007.

[4] Choi, et al., *Nat. Commun.*, **2014**, *62*, 12137.

## What can they do?

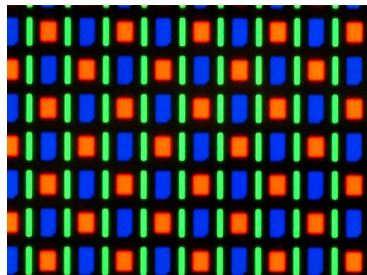
Electrides are powerful reducing agents/have a very low work function.

## Electronics Applications:

- Sodium ion battery anodes<sup>1</sup>
  - Electron injection layers in OLEDs<sup>2</sup>

## Other Physical Properties

- Superconductivity (not high-T)<sup>3</sup>
  - Magnetism<sup>4</sup>



[1] Hu et al., ACS Appl. Mater. Interfaces, 2015, 7, 24016.

[2] Kim et al., *J. Phys. Chem. C*, 2007, 111, 8403.

[3] Miyakawa et al., *J. Am. Chem. Soc.*, 2007, 129, 7270.

[4] Lee et al. *Nat. Commun.* 2020, 11, 1526

[4] Lee et al., *Nat. Commun.*, 2020, 11, 1520.  
Photo courtesy of Matthew Rollings via the Wikimedia Commons

# A Perfect Coalescence

Electrides are a perfect coalescence from the perspectives of theory and application.

- As materials, they are not found in nature, and are thus novel.
- Their ability to act as strong reducing agents can be applied to a variety of applications.
- Their remarkable electronic structure makes them interesting from the theory side.

# Classifying Electrides

There are a few schemes to group electrides with similar character:

## Organic/Inorganic

Organic electrides are usually salts containing alkali metals.

Many inorganic electrides have been synthesized.

## Dimensionality

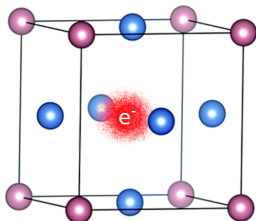
0D, 1D, 2D, 3D

## Stoichiometry

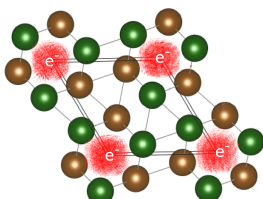
$AE_2Pn$ ,  $M_2C$ ,  $AM(\text{cryptand}-i.j.k)_2$ , etc.

# Dimensionality

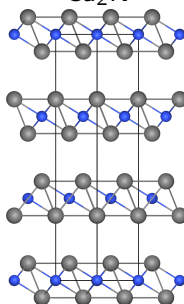
0D Electride:  
 $\text{Ca}_3\text{Pb}$



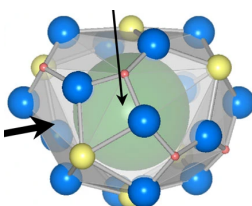
1D Electride:  
 $P6_3/m$  Sodium



2D Electride:  
 $\text{Ca}_2\text{N}$



3D Electride:  
 $\text{Ca}_{24}\text{Al}_{28}\text{O}_{64}$



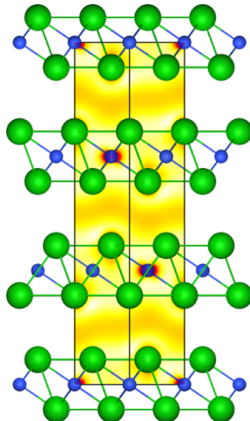
Zhang et al. *J. Mat. Chem. C* 2018 6(3), 575  
Wang et al. *Phys. Rev. B*, 2023, 107(18), 184101  
Toda et al. *Nature* 2013 4(1), 2379

## Layered Electrides

2D Electrides are layered materials where the anionic electron is localized between positively charged sheets.

They can be exfoliated to their monolayers, featuring high surface charge.

These are sometimes called “electrenes.”



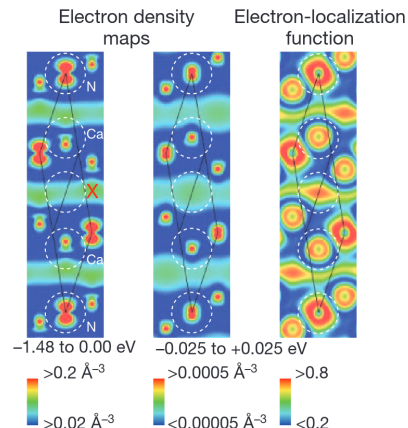
ILDOS plot of  $\text{Ba}_2\text{N}$ , showing 0.5 eV under the Fermi level.

# Dicalcium Nitride

$\text{Ca}_2\text{N}$  was first synthesized in 2002 by reacting  $\text{Ca}_3\text{N}_2$  with Ca metal at high temperature.

Recognized as an electride in 2013 and exfoliated to a monolayer in 2016.

The electride character of  $\text{Ca}_2\text{N}$  was robustly confirmed by a combination of experiment and DFT.



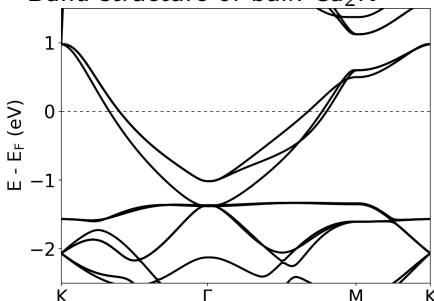
Reckeweg et al., *J. Solid State Sci.*, 2002, 4(5), 575.

Lee et al., *Nature*, 2013, 494, 336.

Druffel et al., *J. Am. Chem. Soc.*, 2016, 138(49), 16089

# Dicalcium Nitride

Band structure of bulk  $\text{Ca}_2\text{N}$



Notable features:

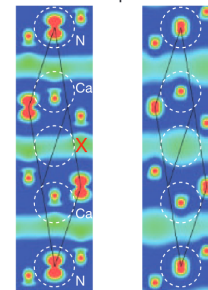
- Metallic
- Minimal DOS around  $E_F$

Reckeweg et al., J. Solid State Sci., 2002, 4(5), 575.

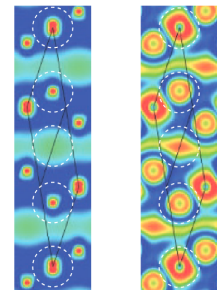
Lee et al., Nature, 2013, 494, 336.

Druffel et al., J. Am. Chem. Soc., 2016, 138(49), 16089

Electron density maps



Electron-localization function



# The AE<sub>2</sub>Pn Electride Class

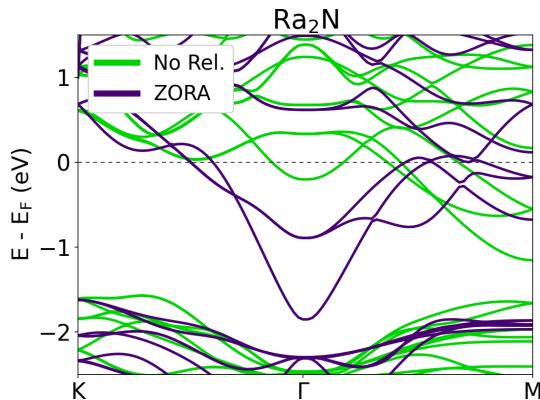
Seven AE<sub>2</sub>Pn electrides in the  $\bar{R}\bar{3}m$  space group have been theorized:

		AE			
		Ca	Sr	Ba	Ra
Pn	N	Ca <sub>2</sub> N	Sr <sub>2</sub> N	Ba <sub>2</sub> N	Ra <sub>2</sub> N?
	P	<del>Ca<sub>2</sub>P</del>	Sr <sub>2</sub> P	Ba <sub>2</sub> P	???
	As	<del>Ca<sub>2</sub>As</del>	<del>Sr<sub>2</sub>As</del>	Ba <sub>2</sub> As	???
	Sb	<del>Ca<sub>2</sub>Sb</del>	<del>Sr<sub>2</sub>Sb</del>	Ba <sub>2</sub> Sb	???

Of these, only the nitrides (Ca<sub>2</sub>N, Sr<sub>2</sub>N, Ba<sub>2</sub>N) are known experimentally.

# A fun thing about $\text{Ra}_2\text{N}$

Relativity governs the occupation of the electride state.



## Other M<sub>2</sub>E Electrides

Transition-metal Carbides ( $R\bar{3}m$ ):

- Y<sub>2</sub>C
- Sc<sub>2</sub>C

Transition-metal Chalcogenides:

- Ti<sub>2</sub>S ( $Pnnm$ )
- Zr<sub>2</sub>S ( $Pnnm$ )
- Hf<sub>2</sub>S<sub>1-x</sub>Se<sub>x</sub> ( $P6_3/mmc$ )

Lanthanide Carbides ( $R\bar{3}m$ ):

- Gd<sub>2</sub>C
- Tb<sub>2</sub>C
- Dy<sub>2</sub>C
- Ho<sub>2</sub>C

Sc<sub>2</sub>C and Al<sub>2</sub>C (theoretical) are semiconducting electrides, where hybridization of the metal and electride states leads to the opening of a band gap.

Introduction  
oooooooooooo

Thermal Expansion  
oooooooooooo

2D Semiconductors  
oooooooooooooooooooo

Conclusions  
o

## Introduction

## Thermal Expansion

## 2D Semiconductors

## Conclusions

## The initial idea

I wanted to know if GGA+D is good enough to model electrides. We narrowed that down to:

*How do the following factors influence the accuracy of DFT on layered electrides compared to experiment?*

- Type of basis set (PAW versus NAO)
- Functional/Dispersion correction
- Thermal expansion

Compare to layered electrides that have been experimentally characterized with XRD at room temperature:  $\text{Ca}_2\text{N}$ ,  $\text{Sr}_2\text{N}$ ,  $\text{Ba}_2\text{N}$ ,  $\text{Sc}_2\text{C}$ ,  $\text{Y}_2\text{C}$ .

# Post-SCF Dispersion Corrections

## Tkatchenko-Scheffler (TS)

$C_6$  coefficients computed by volume-scaling three empirical parameters: polarizability, homoatomic  $C_6$ , and van der Waals radii.

## Many Body Dispersion, Non-Local (MBD-NL)

The polarizabilities are computed using VV10's polarizability functional, and the  $C_6$ s via Casimir-Polder, which are then fed into the CFDM Hamiltonian to compute the dispersion energy.

## Grimme's Dispersion Corrections (D3/D3BJ)

$C_6$  coefficients computed with the Casimir-Polder integral and incorporating their coordination.  $C_8$  coefficients are derived from  $C_6$  by recurrence.

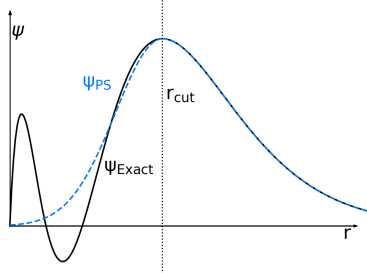
## Exchange-Hole Dipole Moment (XDM)

Includes  $C_6$ ,  $C_8$ , and  $C_{10}$ , capturing higher order interactions. These are derived from the multipole moments of the Hirshfeld-partitioned electron density.

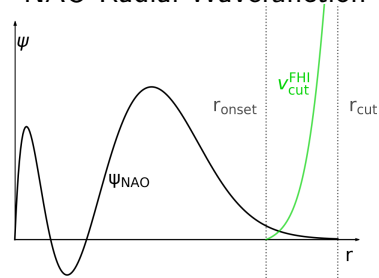
All these dispersion corrections will be paired with PBE, plus B86bPBE-XDM.

# Agreement of Basis Sets: PAW versus NAO

PAW Radial Wavefunction

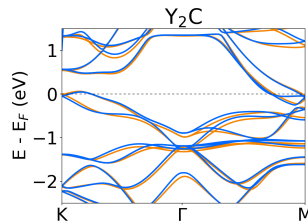
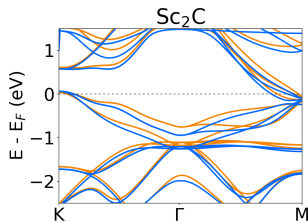
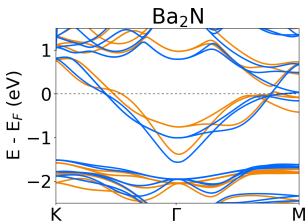
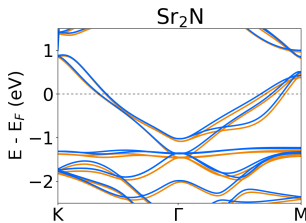
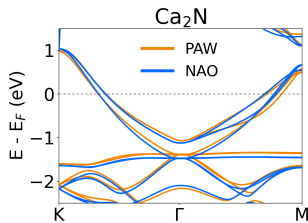


NAO Radial Wavefunction



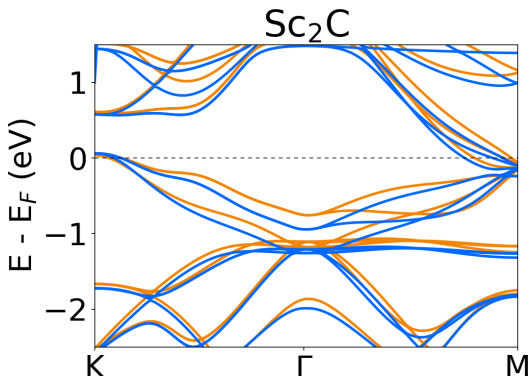
Projector-augmented wave (PAW) bases use planewaves in the regions away from nuclei, so all space is captured by basis functions. Numerical atom-centered orbital (NAO) bases have a finite radial extent, controlled by a cutoff potential. They may struggle to model non-atom-centered features...

# Agreement of Basis Sets

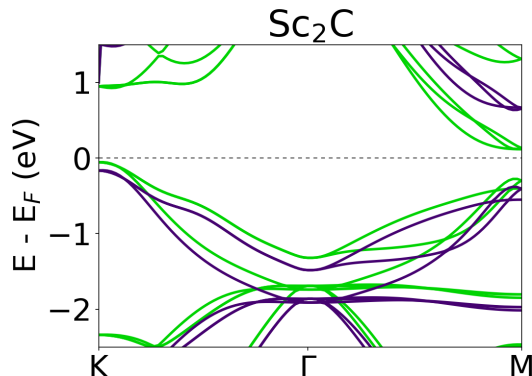


# A Note on $\text{Sc}_2\text{C}$

$\text{Sc}_2\text{C}$  is a small band-gap semiconductor, and GGA functionals tend to shrink band gaps.



Orange: B86bPBE-XDM/PAW  
Blue: B86bPBE-XDM/NAO



Green: HSE06-XDM/NAO  
Purple: PBE0-XDM/NAO

# How do we account for thermal effects?

Most thermal effects in a crystal present as vibrations (phonons).

These can be modeled explicitly (quasi-harmonic approximation)

OR

They can be modeled approximately (Debye approximation)

Suppose that the phonon density of states has a simple form:

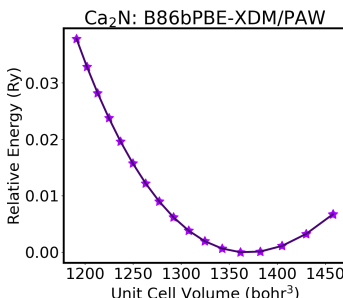
$$g_D(\omega) = \frac{9N\omega^2}{\omega_D^3}, \quad \omega < \omega_D$$
$$3N = \int_0^{\omega_D} g_D(\omega) d\omega$$

$\omega_D$  is the *Debye frequency*, which corresponds to the maximum phonon frequency in the system. The Debye model also assumes that all phonon frequencies are acoustic.

$$\omega = |\mathbf{k}|v_s$$

## Employing the Debye Model

Attain a volume-energy curve for a solid:



The Debye temperature ( $\Theta_D = \hbar\omega_D/k_B$ ) can be approximated as a function of the unit-cell volume and the static Bulk modulus ( $B_{\text{sta.}}$ ).

$$\Theta_D(V) = \frac{f(1/4)}{k_B} \sqrt[3]{6\pi^2 n V^{\frac{1}{2}}} \sqrt{\frac{B_{\text{sta.}}}{M}}$$

The vibrational Helmholtz free energy ( $F_{\text{vib}}$ ) can then be written as a function of  $\Theta_D$ .

$$F_{\text{vib}} = nk_B T \left( \frac{9}{8} \frac{\Theta_D}{T} + 3 \ln \left( 1 - e^{-\Theta_D/T} \right) - D_3 \left( \frac{\Theta_D}{T} \right) \right)$$

$$B_{\text{sta.}} = V \left( \frac{\partial^2 E}{\partial V^2} \right)$$

$$G(V, T) \approx E_{\text{elec}}(V) + F_{\text{vib}}(V, T)$$

# Comparison to QHA

$$\%MAE(X^{\text{pred.}}) = \left( \frac{1}{\bar{X}^{\text{expt.}}} \sum_i \frac{|X_i^{\text{pred.}} - X_i^{\text{expt.}}|}{N} \right) \times 100\%$$

	$c_{\text{th}}$		$V_{\text{th}}$	
	Debye	QHA	Debye	QHA
%MAE (wrt QHA)	0.27	—	0.54	—
%MAE (wrt Expt)	1.82	1.91	3.48	3.34

# Accuracy of Methods

$$\%MAE(X^{\text{pred.}}) = \left( \frac{1}{\bar{X}^{\text{expt.}}} \sum_i \frac{|X_i^{\text{pred.}} - X_i^{\text{expt.}}|}{N} \right) \times 100\%$$

Method	Basis	%MAE			
		$c_0$	$c_{\text{th}}$	$V_0$	$V_{\text{th}}$
B86bPBE-XDM	PAW	1.87	1.82	3.30	3.48
B86bPBE-XDM	NAO	2.06	2.13	4.65	4.70
PBE-XDM	PAW	2.06	2.13	4.90	4.97
PBE-XDM	NAO	2.29	2.30	5.15	5.15
PBE-D3BJ	PAW	2.28	2.51	3.23	3.58
PBE-D3	PAW	2.90	3.16	4.02	4.28
PBE-MBD-NL	NAO	2.25	2.31	5.09	5.15
PBE-TS	NAO	3.09	3.06	6.67	6.56

# Accuracy of Methods

$$\%MAE(X^{\text{pred.}}) = \left( \frac{1}{\bar{X}^{\text{expt.}}} \sum_i \frac{|X_i^{\text{pred.}} - X_i^{\text{expt.}}|}{N} \right) \times 100\%$$

Method	Basis	%MAE			
		$c_0$	$c_{\text{th}}$	$V_0$	$V_{\text{th}}$
B86bPBE-XDM	PAW	1.87	1.82	3.30	3.48
B86bPBE-XDM	NAO	2.06	2.13	4.65	4.70
PBE-XDM	PAW	2.06	2.13	4.90	4.97
PBE-XDM	NAO	2.29	2.30	5.15	5.15
PBE-D3BJ	PAW	2.28	2.51	3.23	3.58
	PAW	2.90	3.16	4.02	4.28
PBE-MBD-NL	NAO	2.25	2.31	5.09	5.15
PBE-TS	NAO	3.09	3.06	6.67	6.56

# Accuracy of Methods

$$\%MAE(X^{\text{pred.}}) = \left( \frac{1}{\bar{X}^{\text{expt.}}} \sum_i \frac{|X_i^{\text{pred.}} - X_i^{\text{expt.}}|}{N} \right) \times 100\%$$

Method	Basis	%MAE			
		$c_0$	$c_{\text{th}}$	$V_0$	$V_{\text{th}}$
B86bPBE-XDM	PAW	1.87	1.82	3.30	3.48
B86bPBE-XDM	NAO	2.06	2.13	4.65	4.70
PBE-XDM	PAW	2.06	2.13	4.90	4.97
PBE-XDM	NAO	2.29	2.30	5.15	5.15
PBE-D3BJ	PAW	2.28	2.51	3.23	3.58
PBE-D3	PAW	2.90	3.16	4.02	4.28
PBE-MBD-NL	NAO	2.25	2.31	5.09	5.15
PBE-TS	NAO	3.09	3.06	6.67	6.56

## Accuracy of Methods

$$\%MAE(X^{\text{pred.}}) = \left( \frac{1}{\bar{X}^{\text{expt.}}} \sum_i \frac{|X_i^{\text{pred.}} - X_i^{\text{expt.}}|}{N} \right) \times 100\%$$

Method	Basis	%MAE			
		$c_0$	$c_{\text{th}}$	$V_0$	$V_{\text{th}}$
B86bPBE-XDM	PAW	1.87	1.82	3.30	3.48
B86bPBE-XDM	NAO	2.06	2.13	4.65	4.70
PBE-XDM	PAW	2.06	2.13	4.90	4.97
PBE-XDM	NAO	2.29	2.30	5.15	5.15
PBE-D3BJ	PAW	2.28	2.51	3.23	3.58
PBE-D3	PAW	2.90	3.16	4.02	4.28
PBE-MBD-NL	NAO	2.25	2.31	5.09	5.15
PBE-TS	NAO	3.09	3.06	6.67	6.56

The small difference between the static and thermally expanded geometries tell us that thermal expansion is very minimal.

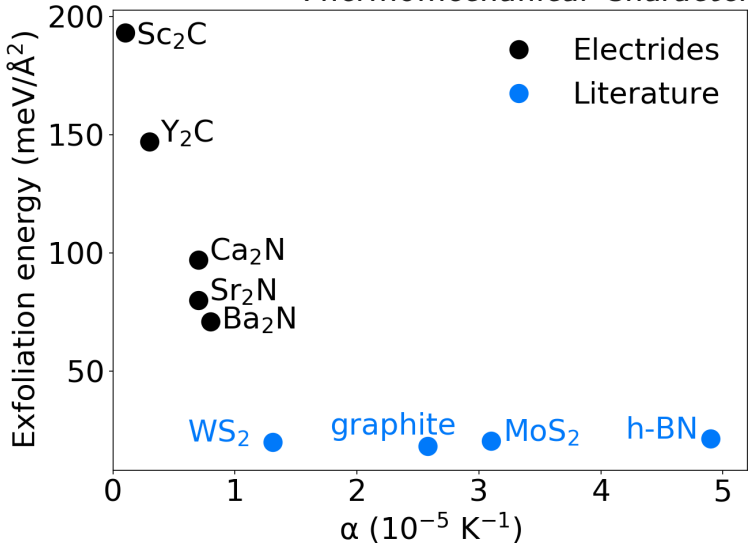
# Exfoliation Energies

Computed with B86bPBE-XDM/PAW:

Electride	$E_{\text{exfol}}^{\text{total}}$ (meV/Å <sup>2</sup> )	Base	Dispersion
Ca <sub>2</sub> N	97	63%	37%
Sr <sub>2</sub> N	80	61%	39%
Ba <sub>2</sub> N	71	55%	45%
Sc <sub>2</sub> C	193	67%	33%
Y <sub>2</sub> C	147	65%	35%

The majority of the interlayer attraction is from the base functional (i.e. electrostatic). Sc<sub>2</sub>C and Y<sub>2</sub>C have two anionic electrons, so have more base contribution. Larger, more polarizable atoms lead to a greater fraction of dispersion.

## Thermomechanical Characteristics



Volumetric coefficient of thermal expansion

$$\alpha = \frac{1}{V} \left( \frac{\partial V}{\partial T} \right)_P$$

## What They Do: Summary

- NAO and PAW basis sets both adequately model the electride state.
- The Debye model is sufficient to model the thermal expansion of layered electrides.
- B86bPBE-XDM/PAW and PBE-D3BJ/PAW were our best-performing methods.
- Thermal expansion is extremely minimal, so it can safely be neglected.
- The small thermal expansion and large exfoliation energies make layered electrides unique among layered materials.

Introduction  
oooooooooooo

Thermal Expansion  
oooooooooooo

2D Semiconductors  
oooooooooooooooooooo

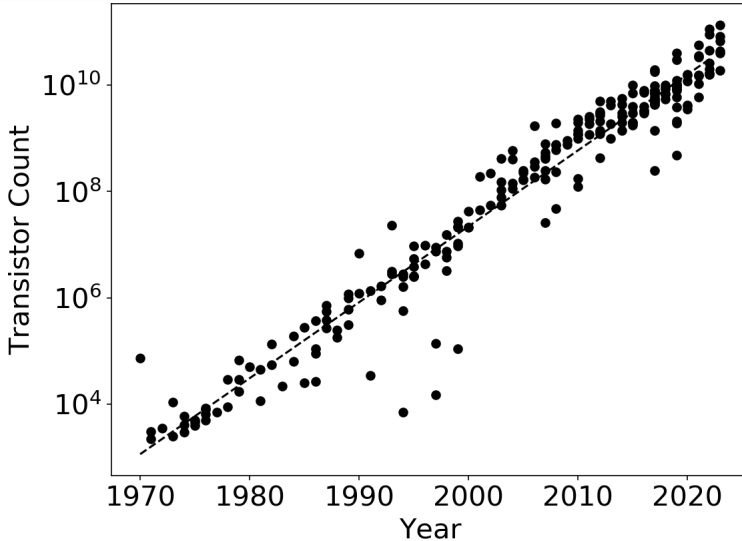
Conclusions  
o

## Introduction

## Thermal Expansion

## 2D Semiconductors

## Conclusions



# The Death of Moore's Law

Moore's law applies to silicon-based transistors.

Pivoting to a new material may be one of the greatest logistical challenges the semiconductor industry will face.

# The Death of Moore's Law

Moore's law applies to silicon-based transistors.

Pivoting to a new material may be one of the greatest logistical challenges the semiconductor industry will face.

A promising alternative to silicon are the transition metal dichalcogenides (TMDCs)

- They feature high mobility, short channel lengths, high on/off ratio, and a small subthreshold swing.

# The Death of Moore's Law

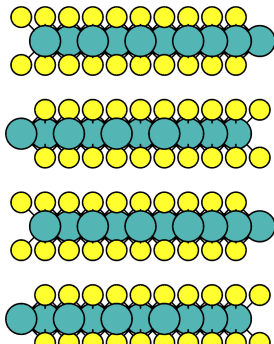
Moore's law applies to silicon-based transistors.

Pivoting to a new material may be one of the greatest logistical challenges the semiconductor industry will face.

A promising alternative to silicon are the transition metal dichalcogenides (TMDCs)

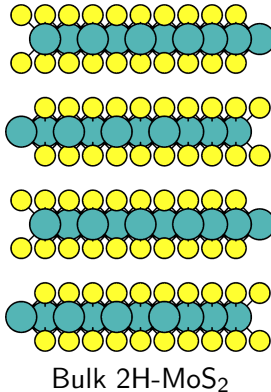
- They feature high mobility, short channel lengths, high on/off ratio, and a small subthreshold swing.

At the front of this class of materials is  $\text{MoS}_2$ .



Bulk 2H-MoS<sub>2</sub>

# Molybdenum Disulfide



- First isolated in 2010.
- Observed in a variety of phases:
  - 1T, 1T', 2H, 3R
- 1T and 1T' are metallic
- 2H and 3R have indirect band gaps.
- Monolayer MoS<sub>2</sub> (1H) has a direct band gap.

Mak *et al.*, *Phys Rev. Lett.*, **2010**, 105, 136805.

# The Contact Resistance Problem

The interface of a metal and a monolayer TMDC tends to exhibit a high contact resistance, *circa*  $1 \text{ k}\Omega \cdot \mu\text{m}$

This can be attributed to:

- Tunneling barriers
- Schottky barriers
- Fermi-level pinning
- Gap state formation
- Sheet resistivity

There is also the issue of semiconductor doping.

## Metal/MoS<sub>2</sub> Junctions

There has been some computational research into the interface properties of the metal/MoS<sub>2</sub> junction.

Kang *et al.* studied Pd, In, Au, Ti, W, and Mo with LDA

Gong *et al.* studied Al, Ag, Ir, Au, Pd, and Pt with LDA+D2

The local density approximation (LDA) already has a tendency to overbind and capture pseudo-dispersion, so its use and the addition of a dispersion correction is will not generally lead to accurate results.

However, both studies noted variance in the interface properties depending on the metal.

Kang *et al.*, *Phys. Rev. X*, **2014**, 4, 031005.

Gong *et al.*, *Nano Lett.*, **2014**, 14, 1714.

# Pn/MoS<sub>2</sub> Junctions

Heavy pnicogen semimetals (Sb, Bi) may be well suited as contact materials for TMDC-based devices.

They have a minimal DOS near the Fermi level, which is unlikely to cause a Schottky barrier.

Contact resistance values:

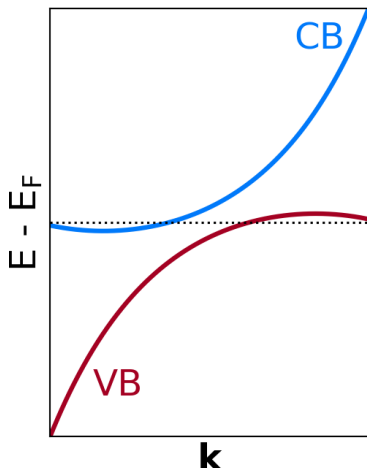
Bi(0001)<sup>1</sup>:  $123 \Omega \cdot \mu\text{m}$

Sb(0112)<sup>2</sup>:  $42 \Omega \cdot \mu\text{m}$

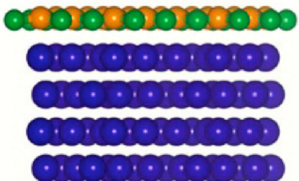
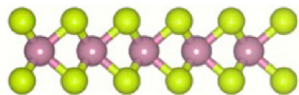
[1] Shen *et al.*, *Nature*, 2021, 593, 211.

[2] Li *et al.*, *Nature*, 2023, 613, 274.

Semimetal band structure:



## Intermediate Materials



Co/h-BN/MoS<sub>2</sub>

Insertion of a h-BN monolayer between a cobalt electrode and MoS<sub>2</sub> was shown to reduce the unfavourable chemical interactions that lead to high contact resistance.

However, this introduces a large tunneling barrier, leading to an experimentally observed contact resistance of  $3 \text{ k}\Omega \cdot \mu\text{m}$ .

Farmanbar and Brocks, *Phys. Rev. B*, **2015**, 91, 161304.

Wang et al., *Adv. Mater.*, **2016**, 28, 8302.

Cui et al., *Nano Lett.*, **2017**, 17, 4781.

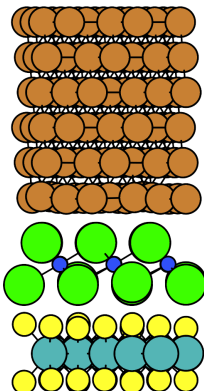
# Electrenes as Intermediate Materials

Electrenes are an excellent material for this application!

- Tunneling barrier free
- Schottky barrier free
- n-doping  $\text{MoS}_2$

Diznab *et al.* studied  $\text{Au}/\text{AE}_2\text{Pn}/\text{MoS}_2$  and  $\text{Cu}/\text{AE}_2\text{Pn}/\text{MoS}_2$  heterostructures for the predicted  $\text{AE}_2\text{Pn}$  electrides ( $\text{Ca}_2\text{N}$ ,  $\text{Sr}_2\text{N}$ ,  $\text{Sr}_2\text{P}$ ,  $\text{Ba}_2\text{N}$ ,  $\text{Ba}_2\text{P}$ ,  $\text{Ba}_2\text{As}$ ,  $\text{Ba}_2\text{Sb}$ )

They concluded that  $\text{Ca}_2\text{N}$  was the best overall choice, thanks to its large surface charge



## The Next Question

Does the metal in a metal/Ca<sub>2</sub>N/MoS<sub>2</sub> heterostructure affect the interface properties?

How does that compare to metal/MoS<sub>2</sub> heterostructures?

# Geometry Metrics

## Intermaterial Separation:

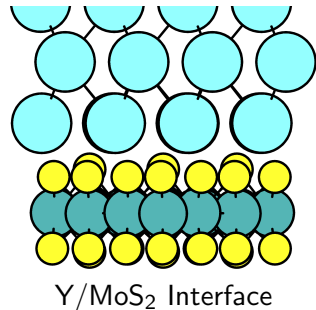
$$\Delta \bar{z}_{S\text{-metal}} = |\bar{z}_S - \bar{z}_{\text{metal}}|$$

The average z-distance between the contact sulfur of MoS<sub>2</sub> and the metal surface.

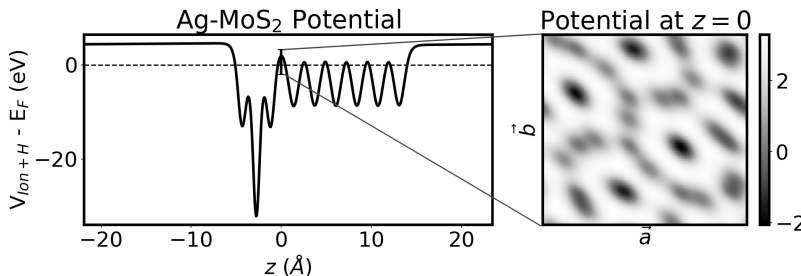
## Interface Distortion:

$$\sigma_{S\text{-metal}} = \sqrt{\sigma_{z,S}^2 + \sigma_{z,\text{metal}}^2}$$

The standard deviation in  $\Delta \bar{z}_{S\text{-metal}}$  representing the distortion at the interface.



# Tunneling Metric



The electrostatic potential of a heterostructure is a 3D function. The  $xy$ -plane average at the metal/MoS<sub>2</sub> junction ( $z = 0$ ) is defined as the tunneling barrier height (TBH).

# Charge Transfer Metrics

## Charge Transfer:

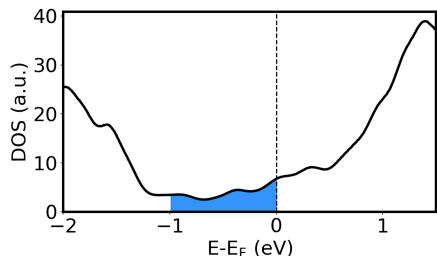
$$Q_{\text{MoS}_2} = Q_{\text{MoS}_2}^{\text{Heterostruc.}} - Q_{\text{MoS}_2}^{\text{Isolated}}$$

Net excess charge on each  $\text{MoS}_2$  formula unit, computed in the QTAIM framework.

## Integrated Gap States:

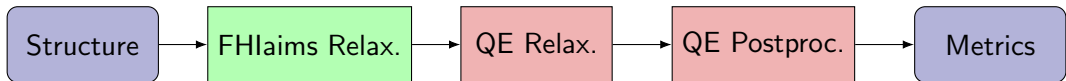
$$\text{IGS} = \frac{1}{A_{\text{cell}}} \int_{E_F - 1 \text{ eV}}^{E_F} D(E) \text{ d}E$$

An integral over the DOS from -1 to 0 eV relative to the Fermi level.



IGS, with the integral shown in blue.

# Geometry Relaxation and Processing Method



PBE-XDM

FHIaims:

- lightdense basis set

Quantum ESPRESSO:

- 90.0 Ry energy cutoff
- 900.0 Ry density cutoff

# Metal/MoS<sub>2</sub> Heterostructures: Bonding Type

Twelve metal/MoS<sub>2</sub> heterostructures were studied:

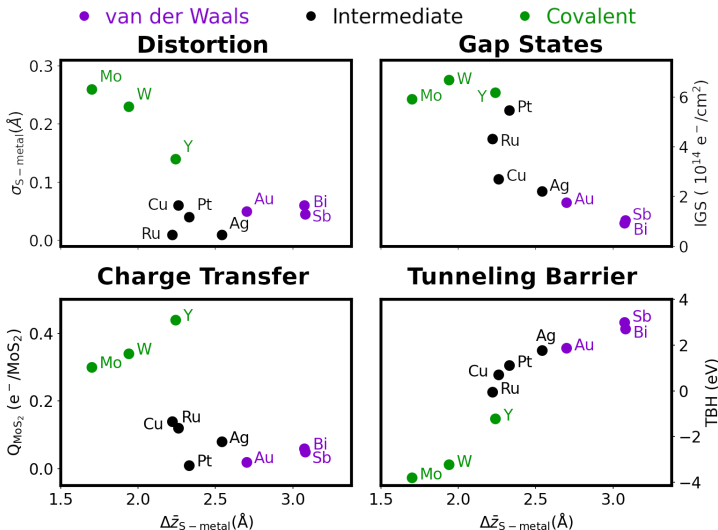
Sb(0001), Sb(011̄2), Bi(0001), Bi(011̄2), Au, Ag, Cu, Pt, Ru, Y, W, Mo

The type of bonding between the materials determines the interface characteristics

An indicator of the bonding type is the average z-distance

- Large  $\Delta z$ : van der Waals
- Medium  $\Delta z$ : intermediate
- Small  $\Delta z$ : covalent

# Metal/MoS<sub>2</sub> Heterostructures: Metrics



# Metal/MoS<sub>2</sub> Heterostructures: Takeaways

Metal/MoS<sub>2</sub> interactions can be classified on a vdW/covalent spectrum.

## van der Waals

- Large  $\Delta z$
- Small  $\sigma_{\text{S-metal}}$
- Small  $Q_{\text{MoS}2}$
- Small gap state formation
- Large tunneling barrier

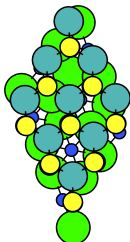
## Covalent

- Small  $\Delta z$
- Large  $\sigma_{\text{S-metal}}$
- Large  $Q_{\text{MoS}2}$
- Large gap state formation
- Small tunneling barrier

# Ca<sub>2</sub>N/MoS<sub>2</sub> Heterostructures

## Geometry A Heterobilayer

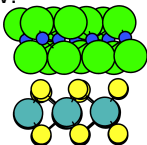
Top view:



Five Ca<sub>2</sub>N/MoS<sub>2</sub> heterobilayers were considered:

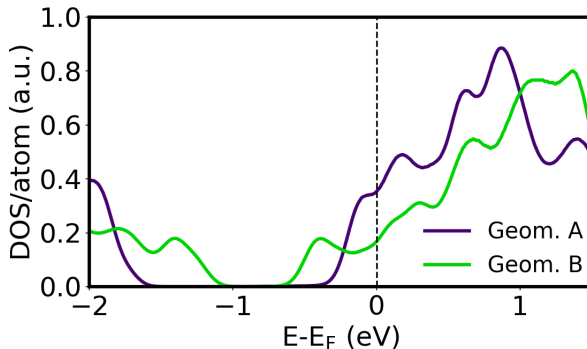
Geometry	$N_{\text{atoms}}$	$\varepsilon_{\text{Ca}_2\text{N}} (\%)$	$Q_{\text{MoS}_2} (\text{e}^-)$
Geom. A	48	0.14	0.35
Geom. B	21	1.67	0.35
Geom. C	87	2.35	0.35
Geom. D	105	4.20	0.36
Geom. E	66	5.23	0.34

Side view:



# Ca<sub>2</sub>N/MoS<sub>2</sub> Heterostructures: Band Gap Shrinking

Geometry	$E_{\text{Gap}}^{\text{MoS}_2}$ (eV)
Geom. A	1.3
Geom. B	0.5
Geom. C	0.9
Geom. D	0.7
Geom. E	0.6



The band gap of MoS<sub>2</sub> is sensitive to strain, but *no strain is applied to the MoS<sub>2</sub> structure.*

## The Geometric Distortion

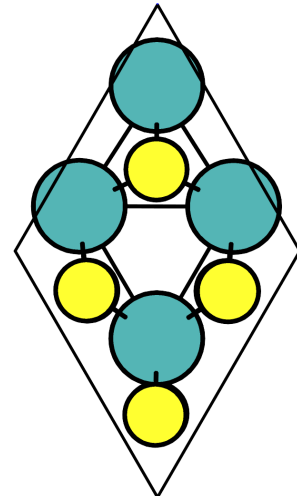
The shrunken band gap is retained when the Ca<sub>2</sub>N is deleted from the structure.

This tells us that this originates from a geometric distortion!

## The Geometric Distortion

The shrunken band gap is retained when the Ca<sub>2</sub>N is deleted from the structure.

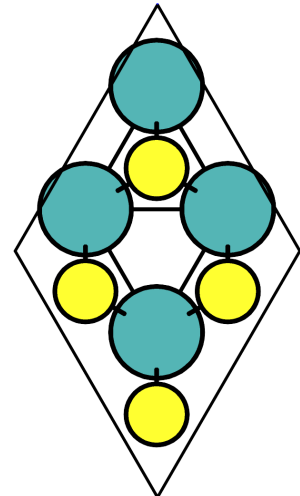
This tells us that this originates from a geometric distortion!



## The Geometric Distortion

The shrunken band gap is retained when the  $\text{Ca}_2\text{N}$  is deleted from the structure.

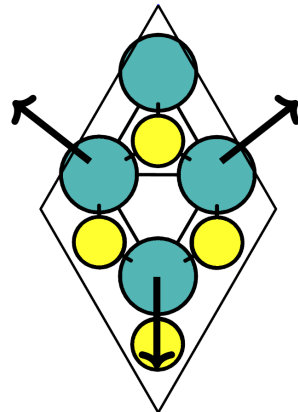
This tells us that this originates from a geometric distortion!



## The Geometric Distortion

The shrunken band gap is retained when the Ca<sub>2</sub>N is deleted from the structure.

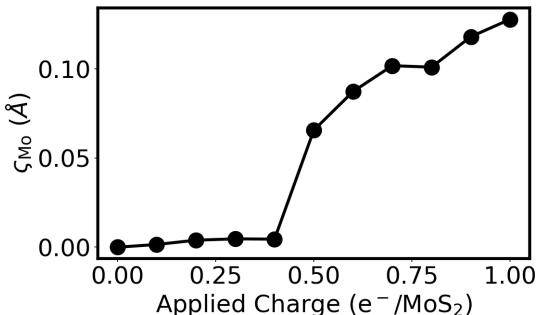
This tells us that this originates from a geometric distortion!



$$\varsigma_{\text{Mo}} = \sqrt{\frac{1}{N} \sum_i \left( d_i^{\text{Mo-Mo}} - d_{\text{pristine}}^{\text{Mo-Mo}} \right)^2}$$

# The Origin(?) of Band Gap Shrinking

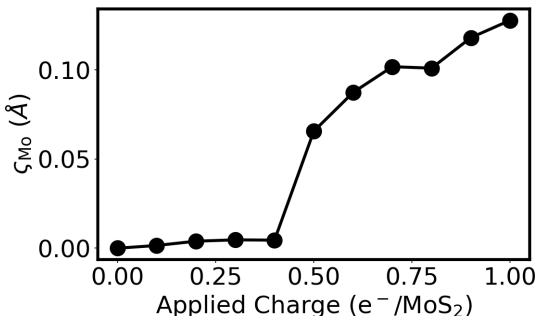
MoS<sub>2</sub> can favour the 1T' phase over 1H given excess negative charge.



MoS<sub>2</sub> spontaneously distorts *circa*  $0.5 e^- / \text{MoS}_2$

# The Origin(?) of Band Gap Shrinking

$\text{MoS}_2$  can favour the 1T' phase over 1H given excess negative charge.



$\text{MoS}_2$  spontaneously distorts *circa*  $0.5 e^-/\text{MoS}_2$

But that is *less* than all of the  $\text{Ca}_2\text{N}/\text{MoS}_2$  Geometries! ( $0.35 e^-/\text{MoS}_2$ )

## $\varsigma_{\text{Mo}}$ for Metal/MoS<sub>2</sub>

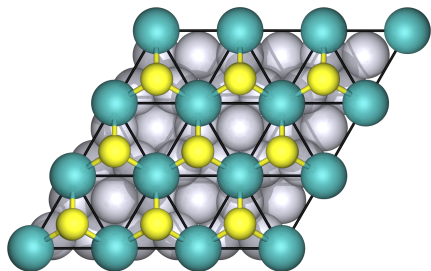
Metal/MoS <sub>2</sub>	$\varsigma_{\text{Mo}}$ (Å)	$Q_{\text{MoS}_2}$ (e <sup>-</sup> /MoS <sub>2</sub> )
Sb(0001)/MoS <sub>2</sub>	0.00	0.04
Sb(011̄2)/MoS <sub>2</sub>	0.00	0.06
Bi(0001)/MoS <sub>2</sub>	0.03	0.02
Bi(011̄2)/MoS <sub>2</sub>	0.00	0.08
Au/MoS <sub>2</sub>	0.00	0.02
Ag/MoS <sub>2</sub>	0.00	0.08
Cu/MoS <sub>2</sub>	0.01	0.12
Pt/MoS <sub>2</sub>	0.00	0.01
Ru/MoS <sub>2</sub>	0.01	0.14
Y/MoS <sub>2</sub>	0.18	0.44
W/MoS <sub>2</sub>	0.04	0.34
Mo/MoS <sub>2</sub>	0.03	0.30

For most metal/MoS<sub>2</sub> interfaces,  $\varsigma_{\text{Mo}}$  is small.

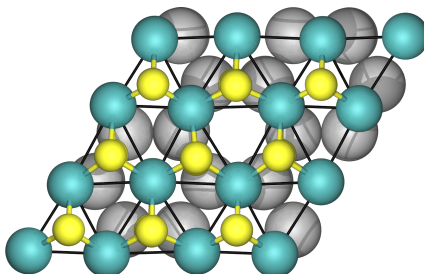
## $\varsigma_{\text{Mo}}$ for Metal/MoS<sub>2</sub>

Metal/MoS <sub>2</sub>	$\varsigma_{\text{Mo}}$ (Å)	$Q_{\text{MoS}_2}$ (e <sup>-</sup> /MoS <sub>2</sub> )	
Sb(0001)/MoS <sub>2</sub>	0.00	0.04	
Sb(011̄2)/MoS <sub>2</sub>	0.00	0.06	
Bi(0001)/MoS <sub>2</sub>	0.03	0.02	For most metal/MoS <sub>2</sub> interfaces, $\varsigma_{\text{Mo}}$ is small.
Bi(011̄2)/MoS <sub>2</sub>	0.00	0.08	
Au/MoS <sub>2</sub>	0.00	0.02	
Ag/MoS <sub>2</sub>	0.00	0.08	Only Y/MoS <sub>2</sub> has a large $\varsigma_{\text{Mo}}$ .
Cu/MoS <sub>2</sub>	0.01	0.12	The isolated, distorted MoS <sub>2</sub> from that interface also has a shrunken band gap.
Pt/MoS <sub>2</sub>	0.00	0.01	
Ru/MoS <sub>2</sub>	0.01	0.14	
Y/MoS <sub>2</sub>	0.18	0.44	
W/MoS <sub>2</sub>	0.04	0.34	
Mo/MoS <sub>2</sub>	0.03	0.30	

## Symmetry Breaking



Pt/MoS<sub>2</sub>



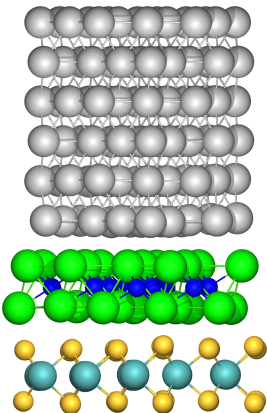
Y/MoS<sub>2</sub>

MoS<sub>2</sub> conforms to the top layer of Yttrium atoms. Large charge transfer may permit this effect.

The same symmetry breaking is observed in Ca<sub>2</sub>N/MoS<sub>2</sub> Geometries B-E.

# Metal/Ca<sub>2</sub>N/MoS<sub>2</sub> Heterostructures

How does the insertion of a Ca<sub>2</sub>N monolayer affect the metal/MoS<sub>2</sub> junction?

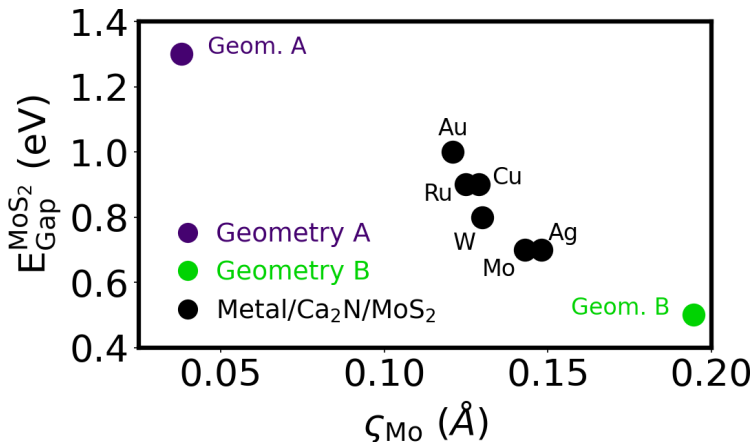


Six metals were considered:  
Cu, Ag, Au, Ru, Mo, W

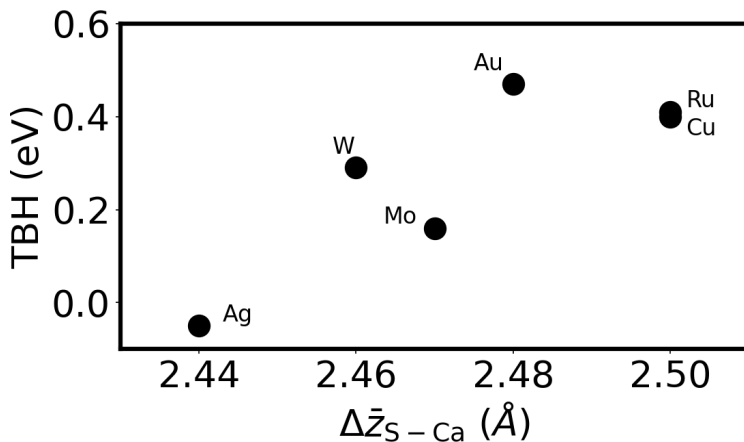
Things to look out for:

- SMo distortion
- Creation of a tunneling barrier
- Variability of metrics w.r.t. metal species

# Metal/Ca<sub>2</sub>N/MoS<sub>2</sub> Heterostructures: $\zeta_{\text{Mo}}$



# Metal/Ca<sub>2</sub>N/MoS<sub>2</sub> Heterostructures: Tunneling Barrier Heights



## Standard Deviations of Metrics

$$\sigma = \sqrt{\frac{1}{N} \sum_i (X_i - \bar{X})^2}$$

Interface	Standard Deviation			
	$\Delta z$ (Å)	$\sigma_{S\text{-metal}}$ (Å)	$Q_{\text{MoS}_2}$ (e <sup>-</sup> /MoS <sub>2</sub> )	TBH (eV)
Metal/MoS <sub>2</sub>	0.37	0.11	0.13	2.48
Metal/Ca <sub>2</sub> N/MoS <sub>2</sub>	0.02	<0.01	0.02	0.20

( $N = 6$ )

Compared to Metal/MoS<sub>2</sub>, Metal/Ca<sub>2</sub>N/MoS<sub>2</sub> interface metrics are only weakly influenced by the choice of the metal.

Introduction  
oooooooooooo

Thermal Expansion  
oooooooooooo

2D Semiconductors  
oooooooooooooooooooo

Conclusions  
o

## Introduction

## Thermal Expansion

## 2D Semiconductors

## Conclusions

# LAYERED ELECTRIDES

WHAT THEY ARE:

WHAT THEY DO:

WHAT CAN THEY DO:

# LAYERED ELECTRIDES

WHAT THEY ARE:

- Ionic materials where a localized electron acts as an anion
- 0D, 1D, 2D, 3D
- Electrenes are 2D electride monolayers

WHAT THEY DO:

WHAT CAN THEY DO:

# LAYERED ELECTRIDES

WHAT THEY ARE:

- Ionic materials where a localized electron acts as an anion
- 0D, 1D, 2D, 3D
- Electrenes are 2D electride monolayers

WHAT THEY DO:

- Small thermal expansion, and large exfoliation energies
- GGA+D DFT is adequate to model the structure of bulk layered electrides

WHAT CAN THEY DO:

# LAYERED ELECTRIDES

## WHAT THEY ARE:

- Ionic materials where a localized electron acts as an anion
- 0D, 1D, 2D, 3D
- Electrenes are 2D electride monolayers

## WHAT THEY DO:

- Small thermal expansion, and large exfoliation energies
- GGA+D DFT is adequate to model the structure of bulk layered electrides

## WHAT CAN THEY DO:

- Enable low resistance contacts to 2D semiconductors
- Introduce flexibility in the choice of metals for those junctions